Trajectory Tracking Control of an Aerial Robot with Obstacle Avoidance

Ícaro Bezerra Viana * **Igor Afonso Acampora Prado** *
Davi Antônio dos Santos * **Luiz Carlos Sandoval Góes** *

* *Technological Institute of Aeronautics, São José dos Campos, SP 12228-900 Brazil (e-mail: icaro,igorap,davists,goes@ita.br).*

Abstract: The present paper deals with the problem of position control of a flying robot type multirotor helicopter with obstacle avoidance. In order to solve the problem, an architecture with model predictive controller (MPC) minimize the tracking error, where are implemented the inclusion of convex constraints on the position vector, making it possible to avoid obstacles with a flexible trajectory. The proposed method is evaluated on the basis of computational simulations considering that the vehicles is subject to disturbance forces. Simulation results show the effectiveness of the method related to the tracking performance with focus on the treatment of obstacle avoidance constraints.

Keywords: Aerial robotics, Multirotor helicopter, Model predictive control, Tracking control, Obstacle avoidance.

1. INTRODUCTION

There is a tendency in using multirotors helicopters as robotics platforms for executing missions in urban areas, for example product delivering and traffic monitoring. In order to continue improving the flight safety and for completely autonomous operation, it is indispensable that the multirotors have incorporated in their control system the ability of avoiding obstacles. The main idea of this topic is to design algorithms able of recognizing the obstacle and recalculating the multirotor trajectory for achieving the final point with safety.

Applications using MPC strategy are expanding to robot control [Vivas and Mosquera, 2005], because this technique is suitable for control of multivariable systems governed by constrained dynamics. The multirotors have an under-actuated dynamics with six degrees of freedom (DOF) and four independent controls. Namely, they have three DOFs of translation and three DOFs of rotation and can be actuated by three torque components and the magnitude of the total thrust vector. To ensure avoidance requirements in the context of trajectory planning, several solutions have been proposed in the literature, such as potential fields [Chuang, 1998, Paul et al., 2008], A^* with visibility graphs [Hoffmann et al., 2008, Latombe, 1991] and mixed integer linear programming (MILP) [Richards and How, 2002]. In particular the latter shows how integer variables are added to the optimization process in order to deal with the constraints properly.

This paper presents a control system for flight of an autonomous multirotors in the presence of obstacles. In order to ensure, simultaneously, performance in the trajectory tracking and treating the obstacle avoidance constraints, a structure with a MPC controller is used for guiding the vehicle. In this, the design of a position controller consists of a linear state-space model predictive control (MPC) strategy. Thus, is used here the trajectory control proposed in [Prado and Santos, 2013], where the controller is designed taking into account a conical constraint on the total thrust vector, ie constraints on the inclination of the rotor plane and on the magnitude of the total thrust vector. This paper extends the problem treated in [Prado and Santos, 2013] and in Santos et al. [2013] including integer constraints on the problem formulation using a quadratic cost function, resulting in a MIQP (mixed-integer quadratic program). The main contribution of this paper is the incorporation of a MIQP form in a predictive control scheme to treat the obstacle avoidance problem for multirotors helicopters.

Figure 1 shows the block diagram of a control system for controlling only the three-dimensional position $\mathbf{r} \in \mathbb{R}^3$ of a multirotor to follow a time-varying position command $\mathbf{r}_\mathrm{d} \in \mathbb{R}^3$. This system is organized in two loops: an inner loop for attitude control and an outer loop for position control. The Navigation System block is responsible for estimating the vehicle's attitude $\mathbf{D} \in \mathrm{SO}(3)$, angular velocity $\boldsymbol{\omega} \in \mathbb{R}^3$, position $\mathbf{r}$, and linear velocity $\dot{\mathbf{r}} \in \mathbb{R}^3$. The Attitude Control block receives an attitude command $\mathbf{D}_\mathrm{d} \in \mathrm{SO}(3)$ and produces the control torque $\boldsymbol{\tau} \in \mathbb{R}^3$ to incline the rotor plane with respect to the horizontal plane as desired. The Position Control block has the role of generating the throttle command (command for the total thrust magnitude) $f \in \mathbb{R}$ and the attitude command $\mathbf{D}_\mathrm{d}$ necessary to accelerate the multirotor in such a way to control its position as desired.

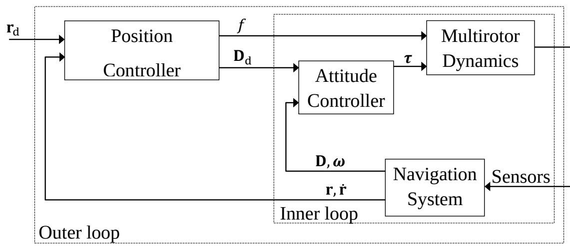

Fig. 1. Block diagram of a multirotor position tracking control system.

The rest of the body text is organized as follows: Section II presents the definition of the problem. Section III describes the problem solution. Section IV describes the evaluation based on computer simulations using MATLAB/SIMULINK and Section V contains the conclusions and suggestions for future work.

2. PROBLEM STATEMENT

Consider the multirotor vehicle and the three Cartesian coordinate systems (CCS). In Figure 2 is assumed that the vehicle has a rigid structure. The body CCS $S_B \triangleq \{X_B, Y_B, Z_B\}$ is fixed to the structure and its origin coincides with the center of mass (CM) of the vehicle. The reference CCS $S_R \triangleq \{X_R, Y_R, Z_R\}$ is Earth-fixed and its origin is at point O. Finally, the CCS $S_{R'} \triangleq \{X_{R'}, Y_{R'}, Z_{R'}\}$ is defined to be parallel to S_R, but its origin is shifted to CM. Assume that S_R is an inertial frame.

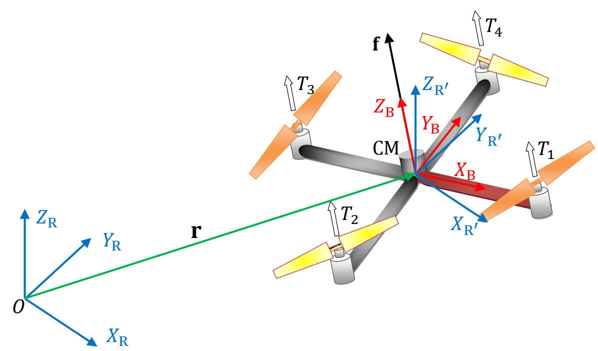

Fig. 2. The Cartesian coordinate systems.

Invoking the second Newton's law and neglecting disturbance forces, the translational dynamics of the multirotor illustrated in Figure 2 can be immediately described in S_R by the following second order differential equation:

$$\ddot{\mathbf{r}} = \frac{1}{m}\mathbf{f} + \begin{bmatrix} 0 \\ 0 \\ -g \end{bmatrix}, \tag{1}$$

where $\mathbf{r} \triangleq [r_x \; r_y \; r_z]^T \in \mathbb{R}^3$ is the position vector of CM, $\mathbf{f} \triangleq [f_x \; f_y \; f_z]^T \in \mathbb{R}^3$ is the total thrust vector, m is the mass of the vehicle, and g is the gravitational acceleration. As illustrated in Figure 2, $\mathbf{f}$ is perpendicular to the rotor plane.

Define the inclination angle $\phi \in \mathbb{R}$ of the rotor plane as the angle between Z_B and $Z_{R'}$. The angle ϕ can thus be expressed by

$$\phi \triangleq \cos^{-1}\frac{f_z}{f}, \tag{2}$$

where $f \triangleq \|\mathbf{f}\|$.

Define the position tracking error $\tilde{\mathbf{r}} \in \mathbb{R}^3$ as

$$\tilde{\mathbf{r}} \triangleq \mathbf{r} - \mathbf{r}_d, \tag{3}$$

where $\mathbf{r}_d \triangleq [r_{d,x} \; r_{d,y} \; r_{d,z}]^T \in \mathbb{R}^3$ is a position command.

Problem 1. Let $\phi_{max} \in \mathbb{R}$ denote the maximum allowable value of ϕ, $f_{min} \in \mathbb{R}$ and $f_{max} \in \mathbb{R}$ denote, respectively, the minimum and maximum allowable values of f. The problem is to find a control law for $\mathbf{f}$ that minimizes $\tilde{\mathbf{r}}$, subject to the inclination constraint $\phi \leq \phi_{max}$, and to the force magnitude constraint $f_{min} \leq f \leq f_{max}$.

Problem 2. Let $\mathbf{L}^l \in \mathbb{R}^3$ and $\mathbf{U}^l \in \mathbb{R}^3$ denote, respectively, the coordinates of the lower left-hand corner and the upper right-hand corner of a static obstacle l. The problem consists in include avoidance requirements so that a control action should calculate a command $\mathbf{f}^{(i)}$ by ensuring that the current position of the ith vehicle $\mathbf{r}^{(i)}$ lie outside the obstacle l, at each time step, as show in Figure 3.

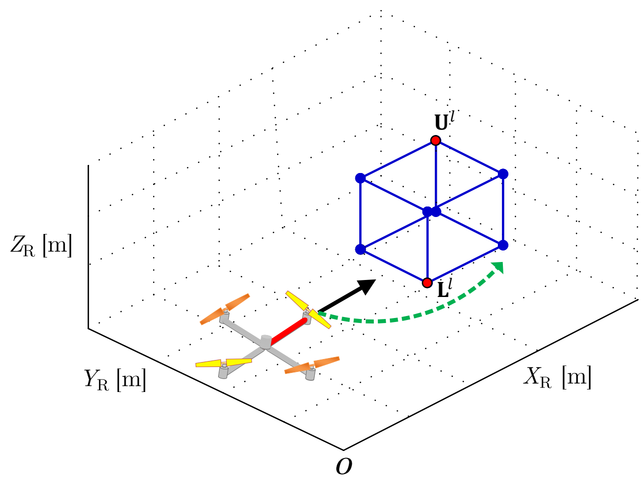

Fig. 3. Obstacle avoidance problem

The obstacles can be modeled in this framework as convex polygons of any number of sides, but, to simplify the presentation, the results in this paper only use cubes, as shows in Figure 3. It supposes that a laser range sensor is used for the detection of the obstacle.

It is assumed that the location of the cube obstacle defined by $\mathbf{L}^l$ and $\mathbf{U}^l$ are known. Thus, to achieve the obstacle avoidance and to attend the requirement proposed simply add the following set of linear inequality convex constraints in the problem formulation,

$$r_x^{(i)} \leq L_x^{(l)} \tag{4}$$
$$or,\ r_x^{(i)} \geq U_x^{(l)} \tag{5}$$
$$r_y^{(i)} \leq L_y^{(l)} \tag{6}$$
$$or,\ r_y^{(i)} \geq U_y^{(l)} \tag{7}$$
$$r_z^{(i)} \leq L_z^{(l)} \tag{8}$$
$$or,\ r_z^{(i)} \geq U_z^{(l)} \tag{9}$$

where $\mathbf{r}^{(i)}$ is the manipulated variable of the optimization process that integrates the MPC controller. These constraints can be represented by the following mixed-integer form by introducing binary variables [Williams and Brailsford, 1996]:

$$r_x^{(i)} \leq L_x^{(l)} + Mb_1^{(il)} \tag{10}$$
$$and,\ -r_x^{(i)} \leq -U_x^{(l)} + Mb_2^{(il)} \tag{11}$$
$$r_y^{(i)} \leq L_y^{(l)} + Mb_3^{(il)} \tag{12}$$
$$and,\ -r_y^{(i)} \leq -U_y^{(l)} + Mb_4^{(il)} \tag{13}$$
$$r_z^{(i)} \leq L_z^{(l)} + Mb_5^{(il)} \tag{14}$$
$$and,\ -r_z^{(i)} \leq -U_z^{(l)} + Mb_6^{(il)} \tag{15}$$

$$and, \quad \sum_{p=1}^{6} b_p \leq 5 \tag{16}$$

A set of binary variables b_p was added to the problem at each time step. The variable M denote an arbitrary positive number, larger than any distance in the problem.

This process can be extended to a general number of time steps, vehicles and obstacles, considering the number of dimensions $N = 3$ and n equal to x, y, or z. The binary variables $b_p^{(il)}$ are the switches, with $p \in [1, ..., 2N]$, corresponding to being on one two sides of the obstacle in each of N dimensions. The complete formulation is,

$$\forall i, \forall l, \forall k \in [1, ..., T-1]: \quad r_n^{(i)}(k) \geq U_n^l - Mb_n^{(il)}(k), \quad \forall n \tag{17}$$
$$and, \quad r_n^{(i)}(k) \leq L_n^l - Mb_{n+N}^{(il)}(k), \quad \forall n \tag{18}$$
$$and, \quad \sum_{p=1}^{2N} b_p^{(il)}(k) \leq 2N - 1 \tag{19}$$

The new constraints in (17-19) are linear in the decision variables, and so the new problem is a MIQP.

3. PROBLEM SOLUTION

The solution to Problem 1 is based on a MPC strategy, described in more details in [Prado and Santos, 2013]. In short, the Problem 1 is solved using a linear state-space model predictive control whose optimization is made handy by replacing the original conic constraint set on the thrust vector by an inscribed pyramidal space, which rendered a linear set of inequalities.

This section proposes a solution to the Problem 2 by inserting linear convex constraints to the optimization problem. Subsection 3.1 describes the system by a discrete-time linear state-space model in the form of incremental control input.

3.1 Incremental-Input State-Space Model

Define the state vector $\mathbf{x} \triangleq [r_\mathrm{x}\ \dot{r}_\mathrm{x}\ r_\mathrm{y}\ \dot{r}_\mathrm{y}\ r_\mathrm{z}\ \dot{r}_\mathrm{z}]^\mathrm{T} \in \mathbb{R}^6$ and the control input vector $\mathbf{u}\,[u_\mathrm{x}\ u_\mathrm{y}\ u_\mathrm{z}]^\mathrm{T} \in \mathbb{R}^3$

$$\mathbf{u} \triangleq \frac{1}{m}\mathbf{f} - \begin{bmatrix} 0 \\ 0 \\ g \end{bmatrix}. \tag{20}$$

Using equation (20), (1) can be immediately rewritten as a continuous-time linear state-space model

$$\dot{\mathbf{x}} = \mathbf{A}\mathbf{x} + \mathbf{B}\mathbf{u}, \tag{21}$$

with

$$\mathbf{A} = \begin{bmatrix} 0&1&0&0&0&0 \\ 0&0&0&0&0&0 \\ 0&0&0&1&0&0 \\ 0&0&0&0&0&0 \\ 0&0&0&0&0&1 \\ 0&0&0&0&0&0 \end{bmatrix} \in \mathbb{R}^{6\times 6} \tag{22}$$

and

$$\mathbf{B} = \begin{bmatrix} 0&0&0 \\ 1&0&0 \\ 0&0&0 \\ 0&1&0 \\ 0&0&0 \\ 0&0&1 \end{bmatrix} \in \mathbb{R}^{6\times 3}. \tag{23}$$

Define the controlled output vector $\mathbf{y} \in \mathbb{R}^3$ to be the position vector, i.e.

$$\mathbf{y} \triangleq \mathbf{C}\mathbf{x}, \tag{24}$$

with

$$\mathbf{C} = \begin{bmatrix} 1&0&0&0&0&0 \\ 0&0&1&0&0&0 \\ 0&0&0&0&1&0 \end{bmatrix} \in \mathbb{R}^{3\times 6}. \tag{25}$$

Let $\mathbf{x}(k) \in \mathbb{R}^6$, $\mathbf{u}(k) \in \mathbb{R}^3$, and $\mathbf{y}(k) \in \mathbb{R}^3$ denote, respectively, the state vector, the control input vector and the controlled output vector, all described in the discrete-time domain. Using the Euler integration method with an integration step of $T_s = 10$ ms, the discretized version of equation (21) and equation (24) is obtained as

$$\begin{array}{ll} \mathbf{x}(k+1) &= \mathbf{A}_\mathrm{d}\mathbf{x}(k) + \mathbf{B}_\mathrm{d}\mathbf{u}(k) \\ \mathbf{y}(k) &= \mathbf{C}_\mathrm{d}\mathbf{x}(k) \end{array}, \tag{26}$$

where

$$\mathbf{A}_\mathrm{d} = \begin{bmatrix} 1&0.01&0&0&0&0 \\ 0&1&0&0&0&0 \\ 0&0&1&0.01&0&0 \\ 0&0&0&1&0&0 \\ 0&0&0&0&1&0.01 \\ 0&0&0&0&0&1 \end{bmatrix} \in \mathbb{R}^{6\times 6}, \tag{27}$$

$$\mathbf{B}_\mathrm{d} = \begin{bmatrix} 0.0001 & 0 & 0 \\ 0.01 & 0 & 0 \\ 0 & 0.0001 & 0 \\ 0 & 0.01 & 0 \\ 0 & 0 & 0.0001 \\ 0 & 0 & 0.01 \end{bmatrix} \in \mathbb{R}^{6\times 3}, \tag{28}$$

and $\mathbf{C}_\mathrm{d} \in \mathbb{R}^{3\times 6}$ remains equal to $\mathbf{C}$.

Consider the discrete-time state-space model of equation (10). It can be rewritten in the incremental-input form as Maciejowski [2002],

$$\begin{aligned} \boldsymbol{\xi}(k+1) &= \tilde{\mathbf{A}}\boldsymbol{\xi}(k) + \tilde{\mathbf{B}}\Delta\mathbf{u}(k) \\ \mathbf{y}(k) &= \tilde{\mathbf{C}}\boldsymbol{\xi}(k) \end{aligned}, \tag{29}$$

with

$$\boldsymbol{\xi}(k) = \begin{bmatrix} \Delta\mathbf{x}(k) \\ \mathbf{y}(k) \end{bmatrix} \in \mathbb{R}^9, \tag{30}$$

$$\tilde{\mathbf{A}} = \begin{bmatrix} \mathbf{A}_\mathrm{d} & \mathbf{0}_{6\times 3} \\ \mathbf{C}_\mathrm{d}\mathbf{A}_\mathrm{d} & \mathbf{I}_3 \end{bmatrix} \in \mathbb{R}^{9\times 9}, \tag{31}$$

$$\tilde{\mathbf{B}} = \begin{bmatrix} \mathbf{B}_\mathrm{d} \\ \mathbf{C}_\mathrm{d}\mathbf{B}_\mathrm{d} \end{bmatrix} \in \mathbb{R}^{9\times 3}, \tag{32}$$

and

$$\tilde{\mathbf{C}} = [\mathbf{0}_{3\times 6}\ \mathbf{I}_3] \in \mathbb{R}^{3\times 9}, \tag{33}$$

where $\Delta\mathbf{x}(k) \triangleq \mathbf{x}(k) - \mathbf{x}(k-1) \in \mathbb{R}^6$ denotes the incremental state vector, $\Delta\mathbf{u}(k) \triangleq \mathbf{u}(k) - \mathbf{u}(k-1) \in \mathbb{R}^3$ is the incremental control input vector, $\mathbf{I}_3$ represents an identity matrix with dimensions 3×3, and $\mathbf{0}_{3\times 6}$ is a matrix of zeros with dimension 3×6.

3.2 Prediction Model

Using equation (29), the prediction model can be obtained as (see Maciejowski [2002], p.50)

$$\hat{\mathbf{y}}_N = \mathbf{G}\Delta\hat{\mathbf{u}}_M + \mathbf{F}, \tag{34}$$

where $\hat{\mathbf{y}}_N \in \mathbb{R}^{3N\times 1}$ stacks the controlled outputs along a prediction horizon of length N, $\Delta\hat{\mathbf{u}}_M \in \mathbb{R}^{3M\times 1}$ stacks the incremental control inputs along a control horizon of length M,

$$\mathbf{G} = \begin{bmatrix} \tilde{\mathbf{C}}\tilde{\mathbf{B}} & \mathbf{0}_{3\times 3} & \dots & \mathbf{0}_{3\times 3} \\ \tilde{\mathbf{C}}\tilde{\mathbf{A}}\tilde{\mathbf{B}} & \tilde{\mathbf{C}}\tilde{\mathbf{B}} & \dots & \mathbf{0}_{3\times 3} \\ \vdots & \vdots & \ddots & \vdots \\ \tilde{\mathbf{C}}\tilde{\mathbf{A}}^{M-1}\tilde{\mathbf{B}} & \tilde{\mathbf{C}}\tilde{\mathbf{A}}^{M-2}\tilde{\mathbf{B}} & \dots & \tilde{\mathbf{C}}\tilde{\mathbf{B}} \\ \vdots & \vdots & & \vdots \\ \tilde{\mathbf{C}}\tilde{\mathbf{A}}^{N-1}\tilde{\mathbf{B}} & \tilde{\mathbf{C}}\tilde{\mathbf{A}}^{N-2}\tilde{\mathbf{B}} & \dots & \tilde{\mathbf{C}}\tilde{\mathbf{A}}^{N-M}\tilde{\mathbf{B}} \end{bmatrix} \in \mathbb{R}^{3N\times 3M} \tag{35}$$

and

$$\mathbf{F} = \begin{bmatrix} \tilde{\mathbf{C}}\tilde{\mathbf{A}} \\ \tilde{\mathbf{C}}\tilde{\mathbf{A}}^2 \\ \vdots \\ \tilde{\mathbf{C}}\tilde{\mathbf{A}}^\mathrm{N} \end{bmatrix} \boldsymbol{\xi}(k) \in \mathbb{R}^{3N}. \tag{36}$$

3.3 Obstacle Avoidance

Consider the following linear convex inequality constraint in matrix form, according to (4-9),

$$\mathbf{U}^l \leqslant \mathbf{r}^{(i)} \leqslant \mathbf{L}^l \tag{37}$$

The above constraints are employed in this work to avoid that the multirotor (i) collides with the static obstacle (l). The vector $\mathbf{L} \triangleq [{L_x}^{(l)}{L_y}^{(l)}{L_z}^{(l)}]^\mathrm{T} \in \mathbb{R}^3$ corresponds to vertex of obstacle with the minimum value of each coordinate of the vehicle. The vector $\mathbf{U} \triangleq [{U_x}^{(l)}{U_y}^{(l)}{U_z}^{(l)}]^\mathrm{T} \in \mathbb{R}^3$ corresponds to vertex of obstacle with the maximum value of each coordinate. Repeating equation (37) along the prediction horizon N, yields,

$$[\mathbf{U}^l]_N \leqslant \mathcal{Y}_N \leqslant [\mathbf{L}^l]_N. \tag{38}$$

Replacing the prediction model (34) into equation (38), and rewriting in terms of the optimization vector $\mathcal{X} \in \mathbb{R}^{(3M+n_dN)}$, with n_d the number of binary variables, one can obtain

$$\mathcal{A}\mathcal{X} \leqslant \gamma \tag{39}$$

where,

$$\mathcal{X} \triangleq \left[\, \Delta\mathcal{U}_M\ b_p^{(il)} \,\right]^\mathrm{T}. \tag{40}$$

and,

$$\mathcal{A} \triangleq \begin{bmatrix} \text{-}\mathbf{G} & -M\mathbf{I}_{\frac{\mathrm{n_d}}{2}\mathrm{N}} & \mathbf{0}_{\frac{\mathrm{n_d}}{2}\mathrm{N}\times\frac{\mathrm{n_d}}{2}\mathrm{N}} \\ \mathbf{G} & \mathbf{0}_{\frac{\mathrm{n_d}}{2}\mathrm{N}\times\frac{\mathrm{n_d}}{2}\mathrm{N}} & -M\mathbf{I}_{\frac{\mathrm{n_d}}{2}\mathrm{N}} \end{bmatrix}, \tag{41}$$

where $\mathcal{A} \in \mathbb{R}^{n_dN\times(3M+n_dN)}$ and the scalar M is a larger positive number previously defined. The vector γ is expressed by,

$$\gamma \triangleq \begin{bmatrix} \mathbf{F} - [\mathbf{U}^l]_N \\ [\mathbf{L}^l]_N - \mathbf{F} \end{bmatrix} \in \mathbb{R}^{n_dN}. \tag{42}$$

which consists in the incremental form of the constraints on the controlled output of the i^{th} vehicle. The matrix $\mathcal{A}$ and the vector γ define linear inequality constraints on the optimization variables.

3.4 Model Predictive Controller

The optimal control vector $\mathbf{u}^*(k)$ computed at the discrete-time instant k is given by $\mathbf{u}^*(k) = \Delta\mathbf{u}^*(k) + \mathbf{u}^*(k-1)$, where $\Delta\mathbf{u}^*(k)$ is the first control vector of $\Delta\mathbf{u}^*_M$, which in turn is obtained by minimizing the following quadratic cost function:

$$J(\Delta\hat{\mathbf{u}}_M) = (\hat{\mathbf{y}}_N - [\mathbf{r}_\mathrm{d}]_N)^\mathrm{T}\,\mathbf{Q}\,(\hat{\mathbf{y}}_N - [\mathbf{r}_\mathrm{d}]_N) + \Delta\hat{\mathbf{u}}_M^\mathrm{T}\mathbf{R}\Delta\hat{\mathbf{u}}_M, \tag{43}$$

subject to the constraints (32).

In this work, the controlled output weighting matrix is assumed to be $\mathbf{Q} = \boldsymbol{\eta} \times \mathbf{I}_{3N}$ and the control input weighting matrix is assumed to be $\mathbf{R} = \boldsymbol{\rho} \times \mathbf{I}_{3M}$.

3.5 Computing Thrust Magnitude and Attitude Commands

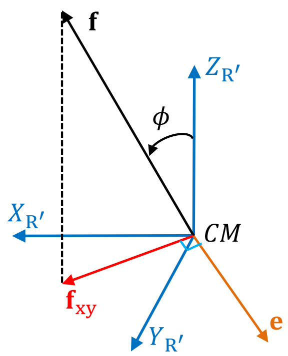

Fig. 4. Relation between the thrust vector $\mathbf{f}$ and its horizontal projection $\mathbf{f}_{\mathrm{xy}}$.

In according to Santos et al. [2013], after computation of the control input $\mathbf{u}$, for implementation purposes, it is necessary to transform it into the corresponding commands of total thrust magnitude (throttle) f and attitude.

Rewrite equation (4) as

$$\begin{bmatrix} f_{\mathrm{x}} \\ f_{\mathrm{y}} \\ f_{\mathrm{z}} \end{bmatrix} = m \begin{bmatrix} u_{\mathrm{x}} \\ u_{\mathrm{y}} \\ u_{\mathrm{z}} + g \end{bmatrix}, \tag{44}$$

whose magnitude f is given by

$$f = m\sqrt{u_{\mathrm{x}}^2 + u_{\mathrm{y}}^2 + (u_{\mathrm{z}} + g)^2}, \tag{45}$$

which is the command for the magnitude of the total thrust $\bar{F}$.

The attitude commands $\bar{D}$ for the internal attitude control loop (see Figure 1) need to be computed from vector $\mathbf{f}$, which has information about the orientation of the plane of rotors with respect the local horizontal. Note that there are infinite attitudes of S_{B} with respect to $S_{\mathrm{R}'}$ for which the Z_{B} axis coincides with $\mathbf{f}$. In order to specify an unique attitude, it is necessary to select a heading angle. For example (since this work is not concerned with heading control), one can choose a zero heading angle, which is equivalent to just taking into consideration the attitude represented by the principal Euler angle/axis $(\phi, \mathbf{e})$, where ϕ is the inclination angle itself and the unit vector $\mathbf{e}$ (see Figure 4) is given by

$$\mathbf{e} = \frac{Z_{\mathrm{R}'} \times \mathbf{f}_{\mathrm{xy}}}{\|Z_{\mathrm{R}'} \times \mathbf{f}_{\mathrm{xy}}\|}, \tag{46}$$

where $\mathbf{f}_{\mathrm{xy}} \triangleq [f_{\mathrm{x}}\ f_{\mathrm{y}}]^{\mathrm{T}}$ denotes the horizontal projection of $\mathbf{f}$. From $(\phi, \mathbf{e})$, this work represent the attitude of S_{B} with respect to S_{R} using direction cosine matrix (DCM) Shuster [1993].

4. SIMULATION RESULTS

The 6DOF dynamics of a multirotor is simulated using the Runge-Kutta 4 as the solver with an integration step of 0.02s. The vehicle's mass is $m = 1$ kg and the gravitational acceleration is assumed to be $g = 9.81$ m/s^2. In order to solve the optimization problem embedded in the MPC algorithm, the branch-and-bound method implemented in the CPLEX software package is taken into account. The following parameterization is adopted for the controller. The control input weights and the controlled output weights are adjusted in $\boldsymbol{\rho} = [0.01\ 0.01\ 0.01]^{\mathrm{T}}$ and $\boldsymbol{\eta} = [1\ 1\ 1]^{\mathrm{T}}$, respectively. The prediction horizon and control horizon are set to $N = 70$ and $M = 5$, respectively. The coordinates of the static obstacle are $\mathbf{L}^l = [1.4\ 1.4\ 1.4]^{\mathrm{T}}$ and $\mathbf{U}_l = [1.9\ 2.5\ 2.9]^{\mathrm{T}}$. The maximum and minimum constraints on the force magnitude are set in $f_{\max} = 20$ N and $f_{\min} = 2$ N, respectively. The attitude controller are proportional-derivative laws tuned so as to make the attitude dynamics have a bandwidth significantly larger than the bandwidth of the position control dynamics.

The position commands chosen for evaluation of the method are trajectories composed by a set of straight lines from the initial position $\mathbf{r}_i = [1\ 1\ 0]^{\mathrm{T}}$ to the final position $\mathbf{r}_f = [5\ 5\ 1]^{\mathrm{T}}$ passing by the waypoints $\mathbf{w}_1 = [1\ 1\ 1]^{\mathrm{T}}$, $\mathbf{w}_2 = [2\ 2\ 2]^{\mathrm{T}}$, $\mathbf{w}_3 = [4\ 2\ 2]^{\mathrm{T}}$, $\mathbf{w}_4 = [5\ 3\ 2]^{\mathrm{T}}$, $\mathbf{w}_5 = [5\ 5\ 2]^{\mathrm{T}}$. Three different speed values are considered: $v = 0.5$ m/s, $v = 1.0$ m/s, and $v = 2.0$ m/s. Concerning the maximum inclination constraint ϕ_{max}, for all speed values, was adopted a value of 30°.

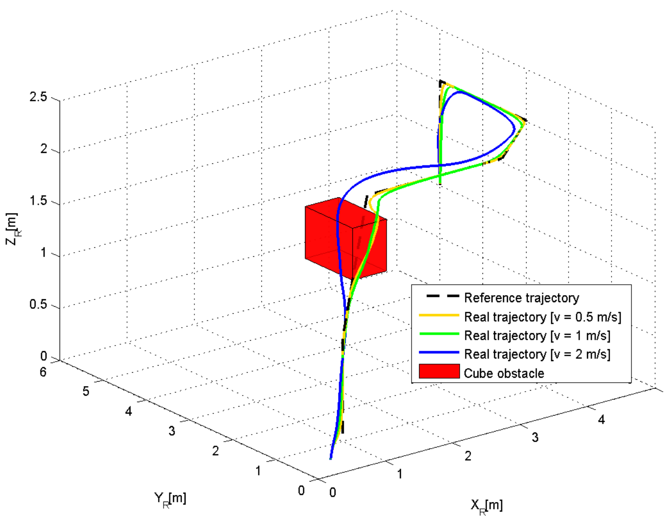

Fig. 5. Trajectory of the multirotor with obstacle avoidance

The simulation results are showed for visualization in Figure 5 and summarized in Table 1. The following figure of merit is used to evaluate the position control error:

$$e_q \triangleq \sqrt{\sum_{k=1}^{k_f} \left(r_{d,n}(k) - r_n^{(i)}(k) \right)^2}, \tag{47}$$

where $r_q^{(i)}(k)$ denotes the i-th realization of $r_q(k)$.

Table 1. Simulation Results for Different Values of v

v m/s	e_x m	e_y m	e_z m
0.5	0.075	0.074	0.065
1.0	0.135	0.132	0.113
2.0	0.235	0.231	0.190

First, one can observe that the control error increases as the speed of the trajectory is increased. For example, for $v = 0.5$ m/s, position errors stay below 8 cm, whereas they approach 23.5 cm when the speed is set to $v = 2.0$ m/s. The main reason is the fact that higher speeds require higher maneuverability and horizontal acceleration to ensure that vehicle follows the reference trajectory in lower time.

To better analyse the method, Figure 6 shows a 2D graphic, for all speeds cases, considering that the obstacle is located in the inner reference trajectory. To validate that the avoidance requirement is attended, is showed the responses when the constraints in MPC are inactive and active, considering that a sustained disturbance force is applied on the system.

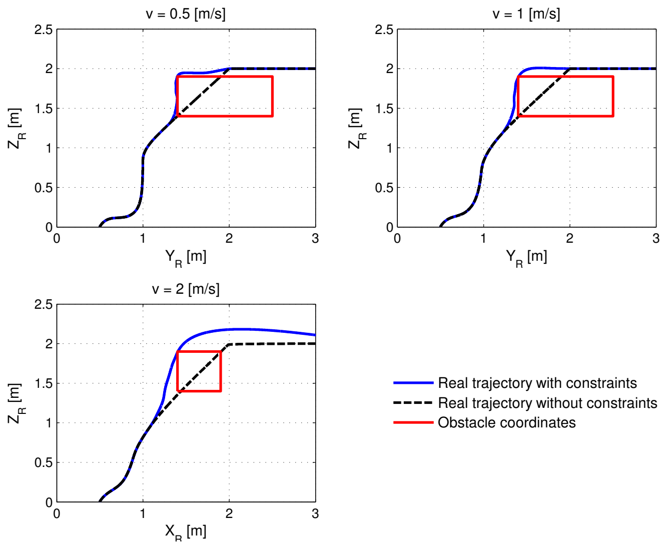

Fig. 6. Obstacle avoidance constraint acting in the vehicle when undergoes disturbance

It is observed that when constraints in MPC are active the controller decides to change the trajectory to avoid the obstacle. The disturbance force is imperceptible during the trajectory because the integral action provided by the incremental model, making the controller able to reject the disturbance force. Note that the selection of the time-step length was appropriate once the incursions of the trajectory do not intersect the obstacle.

5. CONCLUSION

This article discussed the problem of adding position constraints to the formulation from a multirotor position control, so as to ensure obstacle avoidance. The problem was solved using a model predictive controller with a formulation in a mixed-integer quadratic program (MIQP) form. The method was evaluated through computer simulations considering that the vehicle was subjected to disturbances forces to cause change in the trajectory. It is concluded that the proposed method was able to control the multirotor position even under disturbance forces, making then this method, a good solution for control in indoor environment. For a future work, different types of trajectories will be investigated and a hardware-in-the-loop (HIL) environment will be used for experimental evaluation of the proposed method.

ACKNOWLEDGEMENTS

The authors would like to thank the Conselho Nacional de Desenvolvimento Científico e Tecnológico (CNPq) and the Instituto Tecnológico de Aeronáutica (ITA) by the necessary support to realize the present work.

REFERENCES

J. H. Chuang. "Potential-based modeling of threedimensional workspace for obstacle avoidance." *IEEE Transactions on Robotics and Automation,* 14(5):778785, 1998.

G.M. Hoffmann, S.L. Waslander, and C.J. Tomlin. "Quadrotor helicopter trajectory tracking control." *Proc. AIAA Guidance, Navigation, and Control Conf.,* Honolulu, HI, 2008.

J.C. Latombe. "Visibility Graph Method." *Kluwer academic publishers,* 155161, 1991.

J. M. Maciejowski. "Predictive Control with Constraints." *Harlow: Prentice-Hall* (2002)

T. Paul, T.R. Krogstad, and J.T. Gravdahl. "Modelling of UAV formation flight using 3D potential field." *Simulation Modelling Practice and Theory* (16(9):14531462, 2008.)

I. A. A. Prado, D. A. Santos. "Multirotor position tracking using a linear constrained model predictive controller." *22nd International Congress of Mechanical Engineering* (Ribeirão Preto, SP, 2013.)

I. A. A. Prado, D. A. Santos. "A Safe Position Tracking Strategy for Multirotor Helicopters." *22th Mediterranean Conference on Control and Automation (MED)* (Palermo, Italy, 2014.)

A. Richards and J. P. How. "Aircraft trajectory planning with collision avoidance using mixed integer linear programming." *American Control Conference* (2002)

D. A. Santos, O. Saotome. "Trajectory control of multirotor helicopters with thrust vector constraints." *In: 2013 21st Mediterranean Conference on Control & Automation (MED) 2013* (Platanias. 21st Mediterranean Conference on Control and Automation, 2013. p. 375.)

M. Shuster. "A Survey of Attitude Representations." *The Journal of the Astronautical Sciences* (41(4), 1993, 439-517)

A. Vivas, V. Mosquera. "Predictive function control of a PUMA robot." *ACSE Conference* (2005)

H. P. Williams, S. C. Brailsford. "Computational Logic and Integer Programming." *Advances in Linear and Integer Programming,* edited by J. E. Beasley, Clarendon, Oxford, 249-281, 1996.